Stability of Arch Tunnel in Different Magnitude of Earthquake with Effect of Weathering in Western Ghats of India

Zaid Mohammad[1] (0000-0001-6610-8960), Naqvi M. Wasif[2] (0000-0001-9997-8196), Sadique M. R.[3] (0000-0002-9570-6801)

[1,3]Department of Civil Engineering, Aligarh Muslim University, Aligarh, U.P., India
[2]Department of Civil and Environmental Engineering, The University of Toledo, Ohio, USA
mohammadzaid1@zhcet.ac.in

Abstract. Tunnels are the lifeline of modern civilization. With the ongoing scarcity of open ground space, the demand for underground tunnels has increased many folds. Stability of tunnels is influenced by many natural and manmade activities. Earthquake is one of the fiercest natural calamities and like every other structure, tunnels are prone to be affected by it. Past studies show that tunnels in rocks are more stable than in soils during earthquake, but the studies have ignored the weathering of rock with the passage of time. Weathering of rock has a significant effect on its properties and hence the stability of tunnel is affected by it during an earthquake event. The present study aims to analyze the stability of underground rock tunnel affected by weathering phenomenon. An arch tunnel, surrounded by Basalt Rock material undergone weathering, is subjected to four different earthquake events of the past. The rock is modeled using Mohr-Coulomb criteria in a finite element-based software Abaqus. 2D plane stain modeling has been considered for the present study. The absorbing boundary condition has been applied for the earthquake analysis. The stability of tunnel is analyzed by determining the deformation at different depth of overburden. The results of the paper conclude that as the depth of overburden increases, the range of deformation at different locations reduces, thus, showing the effect of lithostatic condition. Also, the deformation increases as the weathering stage of the rock increases for each magnitude of earthquakes. The results also show that as the depth of overburden increases, the weathering has significant effect on the tunnel stability. Finally, it is concluded that, the overburden depth doesn't have much effect on the stability of tunnel under the event of minor earthquakes while the overburden depth proved to be of greater significance in case of major earthquake events.

Keywords: Tunnels; Earthquake; Basalt; Weathering; Abaqus.

1 Introduction

Urbanization is one of the greatest challenges for the fast-growing cities. It has resulted in the increase of population density in many cities. Good transportation network is the backbone of any nation and is known as the key factor for its growth. The rapid urbanization needs wide network of transportation to facilitate public needs such as subways, highways, tunnels etc. Tunnels have been used since historic times for

multiple purposes such as carving roads through hills or to overcome the scarcity of available land space by going underground. Zhang et al. have proposed an analytical solution for the structural response of an existing tunnel to underlying new tunnel [1]. Liu et al. have also proposed an analytical solution to understand the mechanical behavior of the existing tunnel due to excavation below it by taking the variation of coefficient of subgrade modulus [2]. Behavior of existing tunnel due to excavation for new construction of tunnel has also been studied by many researchers [3,4].

Tunnels in rocks are predominant and have been the focus of study from many years [5,6]. The behavior of tunnel is affected by its shape like a circular, rectangle, arch, etc. Arch Tunnels have been studies using analytical, physical and numerical model etc. methodologies [7–10]. With the increase in computational power and complexity of tunnel study, a numerical method is widely used to study tunnel behavior. Structural design failure, landslide, earthquake, sinkholes, etc. are the main causes of tunnel failure. Many tunnel failures were caused due to an earthquake in the past. Lai et al. had carried out finite element analysis of multi-arch tunnel under the seismic event of El Centro earthquake using Johnson-Epstein acceleration time-history curve to generate earthquake event for the model. They have concluded that the horizontal deformation is more than the vertical deformation. Also, the deformations caused by the seismic loading have a great impact on the stability of the tunnel [11].

The studies have been carried out in the past using numerical methods to study the tunnel [12–20]. Do et al. have designed the tunnel lining in multi-layered grounds. They have shown that a reduction of the upward pressure applied on the lower half of the tunnel needs to be considered and there is a significant dependency of the tunnel lining to the position and the thickness of the weaker ground layer [13]. For Twin Tunnels having ground-borne vibrations induced by train movement, the response of both the tunnel should be considered simultaneously for the numerical analysis [15].

Low frequency far field earthquakes is more dangerous as compared to a high frequency near field earthquakes for underwater tunnels [21]. Cheng et al. studied the effect of the bidirectional earthquake on underwater tunnels [22]. Miao et al. carried out the seismic study for the spatially varied ground motion of underwater tunnels and location of seepage and severe damage can be predicted by the proposed method [23]. The study on the layered ground under the oblique earthquake waves has been carried out by Zhao et al. [24]. A new proposal of a second lining has been suggested for Sanyi railway tunnel under the Chi-Chi earthquake loading [25]. Many more researchers have studied the seismic behavior of the tunnels [26-30].

Weathering in rocks is a common phenomenon and is not yet studied in much detail with respect to tunnel stability under seismic loading. The present study deals with the Arch shaped tunnel having 7 m diameter. The tunnel is surrounded by the Basalt rock mass. The stability of tunnel is studied under the effect of four different earthquake loading ranging from minor to major. The effect of weathering of Basalt rock is taken into consideration by modifying the properties of rock taken from experimental data. Also, the depth of the tunnel has been varied to analyze the effect of overburden pressure.

2 Numerical Model

The dynamic analysis has been carried out for the two-dimensional plane strain model of 42m x 42m size using finite element software Abaqus/Dynamic. An arch-shaped tunnel of 7m diameter and tunnel lining of 120 mm thickness is modeled [31]. The three depth 5m, 10m, and 17.5m of overburden has been adopted to compare the effect of overburden depth under different earthquakes for different stages of rock mass weathering. The CPE3R-3-noded plane strain linear triangular element with reduced integration and hourglass control element type has been used for meshing the model. An initial overburden of 500 m of overburden due the already present rock mass has been taken into account in the form of pressure at the top line of the model. The infinite boundary condition has been adopted at the vertical boundary of the tunnel model [31]. The CINPE4-4-noded linear infinite quadrilateral element was used for the infinite boundary condition meshing. 1.5m mesh size has been used for meshing the rock mass and 0.1m for meshing the tunnel lining.

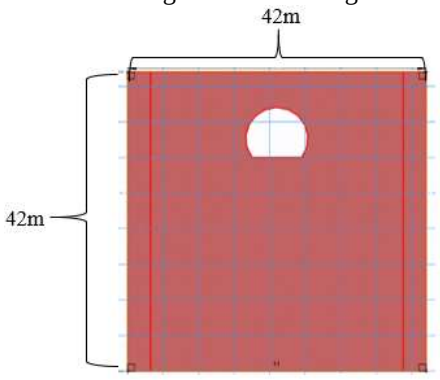

Fig. 1. Geometry of tunnel.

2.1 Input Properties

The Mohr-Coulomb material model has been considered for the behavior of the rock mass. Various properties of different rock mass taken in the present study are shown in Table 1. [32–38,39–41]. The weathering of basalt rock is controlled by changing its properties. The different weathering stages considered in the present study are Fresh Basalt (W0), Slightly Weathered Basalt (W1), Medium Weathered Basalt (W2), and Highly Weathered Basalt (W3).

Table 1. Properties of different weathering Stages [42].

Rockmass	Young's Modulus (GPa)	Poisson's Ratio (v)	Density (kg/m^3)	Friction Angle (°)	Dilation Angle (°)	Cohesion (MPa)
Basalt (W_0)	46.50	0.186	2960	63.38	12	26.25
Basalt (W_1)	20.60	0.260	2740	53.71	12	18.50
Basalt (W_2)	02.80	0.272	2470	33.33	04	08.08
Basalt (W_3)	00.60	0.272	1820	43.87	00	01.64
Concrete	31.6	0.15	2400			

2.2 Analysis

The model was prepared using Abaqus/CAE and boundary conditions were applied. The vertical sides of the model were restrained in position by creating infinite boundary conditions. The earthquake loading has been applied at the base of the model in the form of the acceleration-time history of different earthquakes. The Acceleration vs. time history plot is shown in Figure 2.

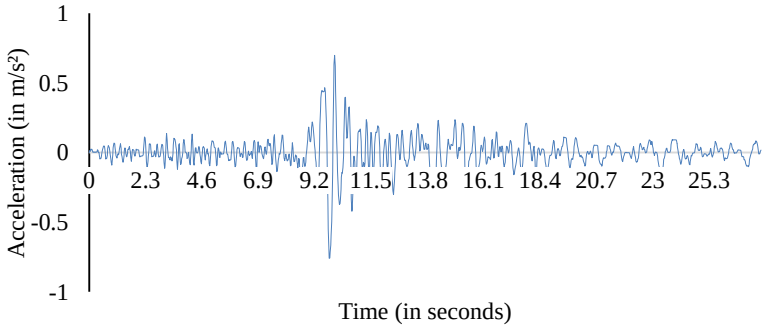

(a) 4.6M

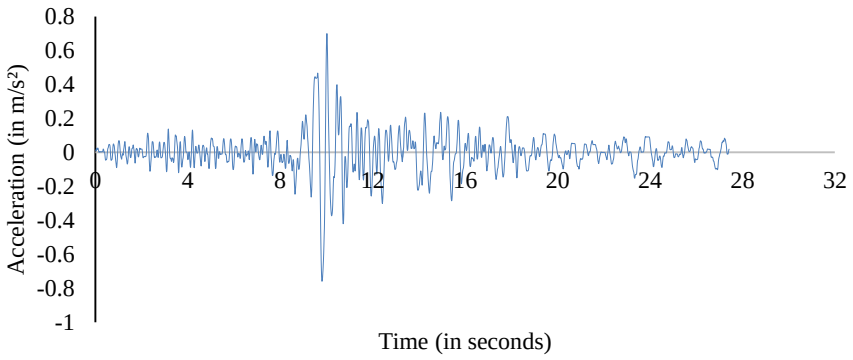

(b) 5.6M

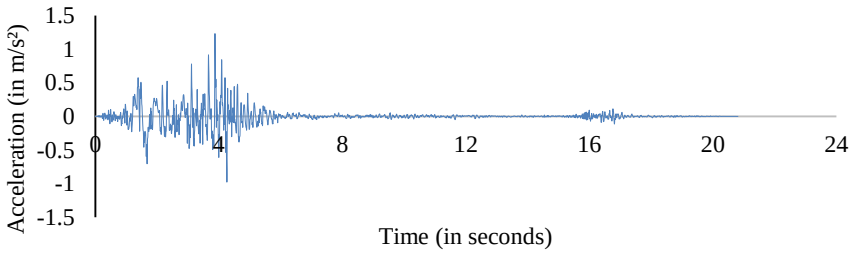

(c) 6.5M

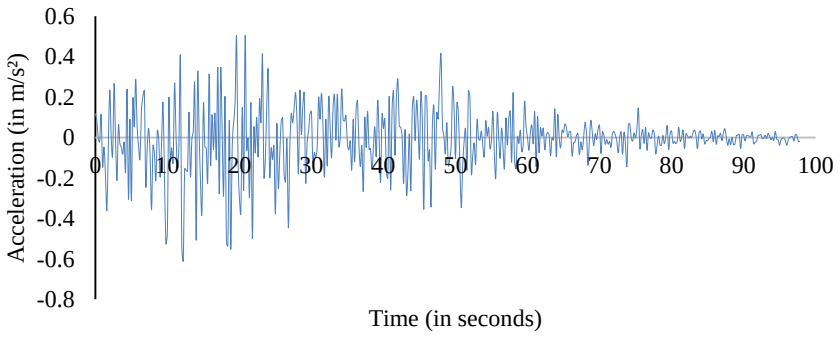

(d) 7.4M

Fig. 2. Earthquake Loading [43]

3 Results and Discussion

The paper deals with the finite element analysis of an arch-shaped tunnel under different earthquake loading subjected to weathering of surrounding rock material at different overburden pressure. Figure 3 shows the deformation of the crucial tunnel points namely crown, left and right springer, and invert of an arch shape tunnel for the different magnitude of earthquakes having a 5m depth of overburden. The invert position is the most deflected one with a magnitude of 1.86 m deflections in the case of the most severe earthquake as shown in Figure 3(d). The deformation of crucial tunnel points tends to increase with the increase in the weathering of rock where fresh basalt rock has the least deflection and highly weather rock has the maximum deflection at all points. Also, as expected the greater the magnitude of earthquake the higher deflection at all the tunnel points as evident from Figure 3(a) to 3(d).

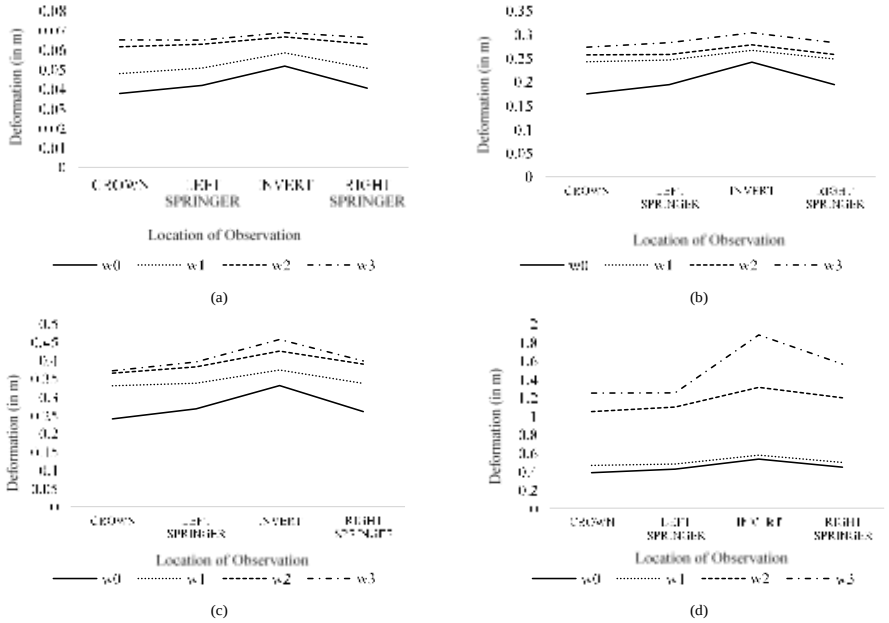

Fig. 3. Deformation at different locations of observation for different weathering stages of rock for 5m overburden for (a) 4.6M, (b) 5.6M, (c)6.5M, and (d) 7.4M magnitude of earthquake.

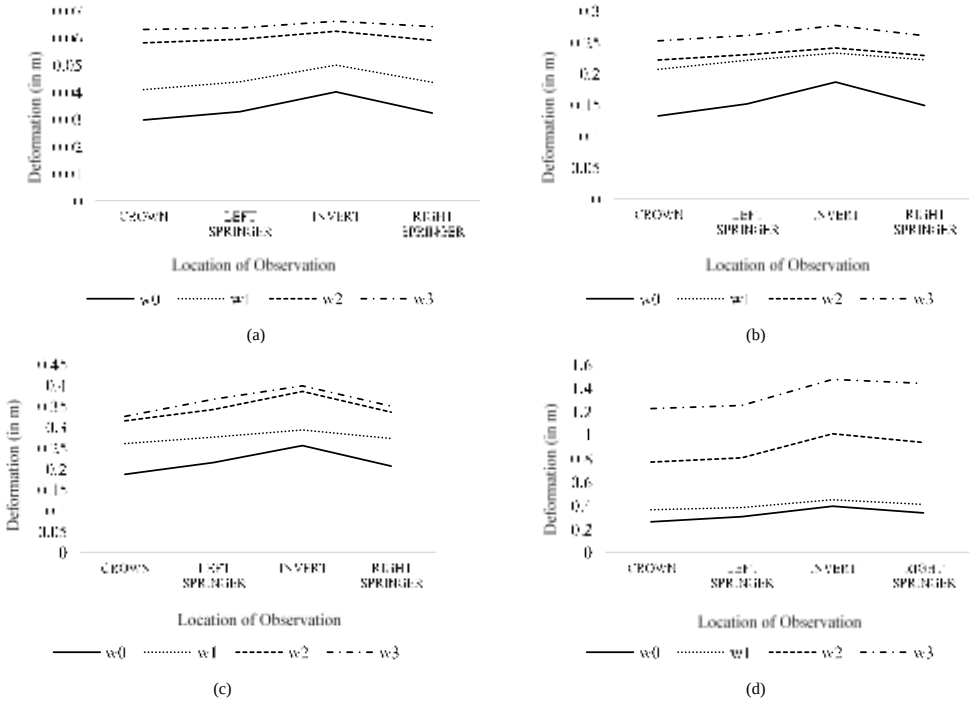

Fig. 4. Deformation at different locations of observation for different weathering stages of rock for 10m overburden for (a) 4.6M, (b) 5.6M, (c)6.5M, and (d) 7.4M magnitude of earthquake.

The deformation of crown, springer, and invert for different stages of weathering is shown in Figure 4 having an overburden depth of 10m. This shows that the highly weathered basalt rock (W3) has maximum deformation by 98% more deformation as compared to fresh basalt rock and the fresh basalt rock (W0) has minimum deformation in case of 4.6M at right springer. Similarly, W3 is 63% more deformed as compared to W1 for 5m depth of overburden and 126% in case of 17.5m depth of overburden for 5.6M, 6.5M, and 7.4M earthquakes. Also, the crown is subjected to minimum deformation and invert has maximum deformation.

Figure 5 shows the variation of deformation at different locations of the tunnel for W0, W1, W2, and W3 stages of weathering at an overburden depth of 17.5m. Comparing Figures 3, 4 and 5, it is evident as the depth of overburden increases, the range of deformation at different locations reduces, thus, showing the effect of lithostatic condition.

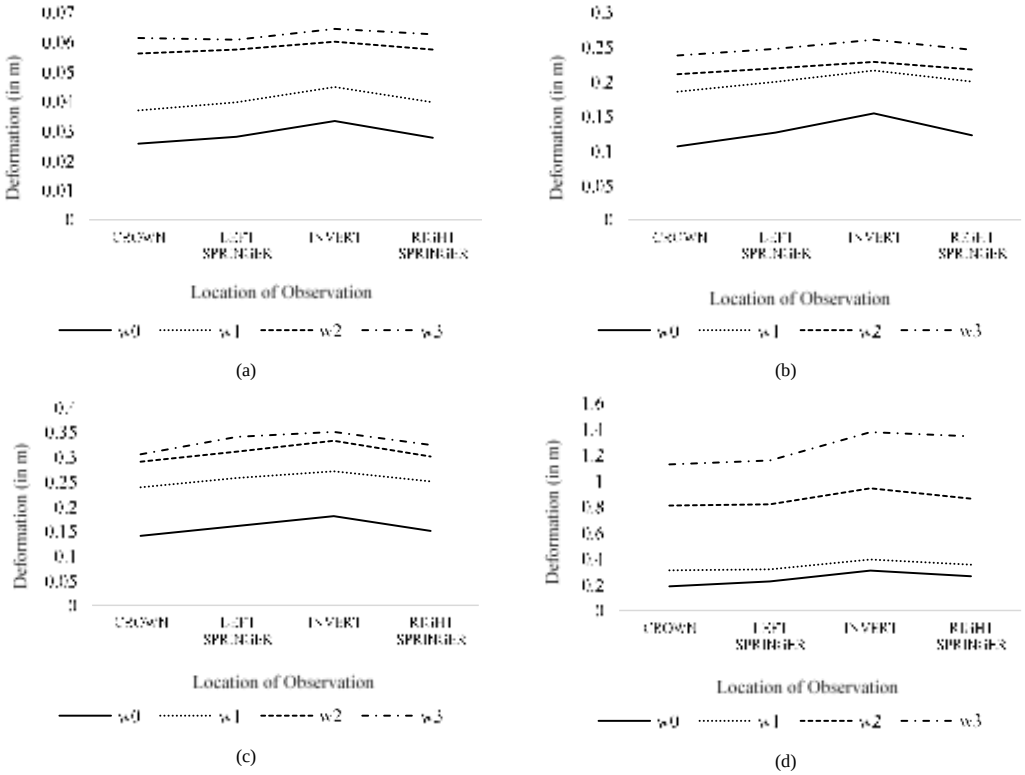

Fig. 5. Deformation at different locations of observation for different weathering stages of rock for 17.5m overburden for (a) 4.6M, (b) 5.6M, (c) 6.5M, and (d) 7.4M magnitude of earthquake.

Figure 6 shows the comparison of different overburden depth in the form of a graph between weathering stages of rock and deformation at the right springer of an arch shape tunnel for the different magnitude of earthquakes. The deformation increases as the weathering of the rock increase with the increase in the magnitude of the earthquake. Also, with the increase in the magnitude of earthquake the difference between the highest and lowest deformation increases. This shows that the effect of the magnitude of the earthquake increases with the increase in deformation.

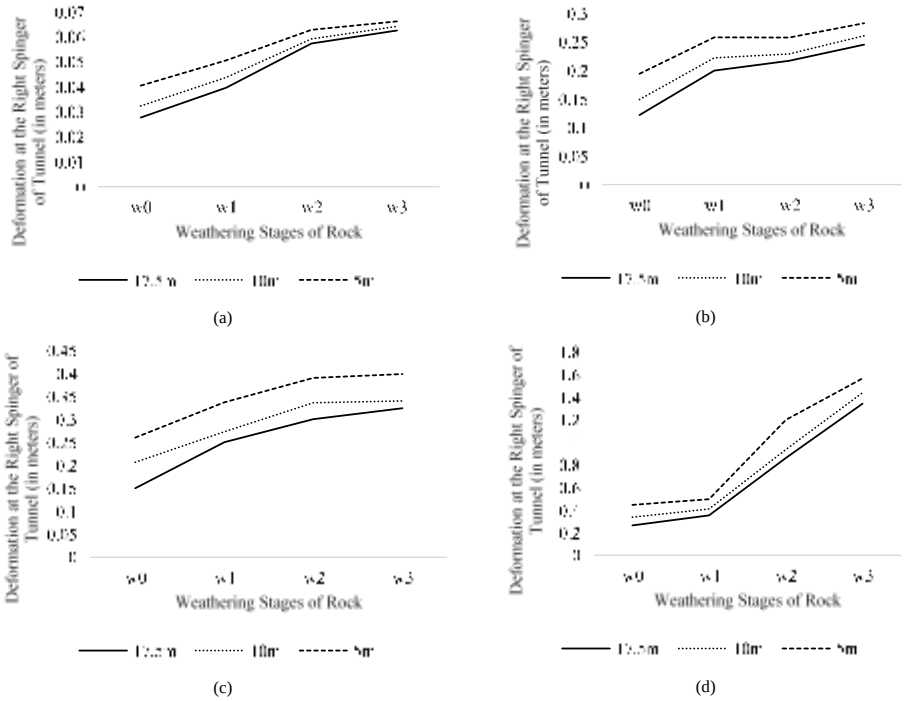

Fig. 6. Comparison of the depth of overburden for different stages of weathering under the varying magnitude of earthquake for deformation at right springer for (a) 4.6M, (b) 5.6M, (c)6.5M, and (d) 7.4M magnitude of earthquake.

In the case of 4.6M earthquake and 17.5m depth of overburden, deformation increases from weathering stage W0 to W3 by 126%, for 10m by 98% and for 5m by 63%. In the case of 5.6M earthquake and 17.5m depth of overburden, deformation increases for weathering stage W0 to W3 by 101%, for 10m by 74% and for 5m by 45%. In the case of 6.4M earthquake and 17.5m depth of overburden, deformation increases for weathering stage W0 to W3 by 115%, for 10m by 64% and for 5m by 53%. In the case of 7.4M earthquake and 17.5m depth of overburden, deformation increases for weathering stage W0 to W3 by 407%, for 10m by 327% and for 5m by 252%. Thus, evidently as the depth of overburden increases, the weathering has a significant effect on the tunnel stability. Also, the higher magnitude earthquakes have much substantial variation of deformation.

Figure 7 shows the comparison of depth of overburden of an arch tunnel for each stage of weathered basalt by plotting a graph between deformation and the magnitude of the earthquake at right springer of the tunnel. This shows that the overburden depth doesn't have much effect on the stability of the tunnel under the event of minor earthquakes while the overburden depth proved to be of greater significance in case of major earthquake events.

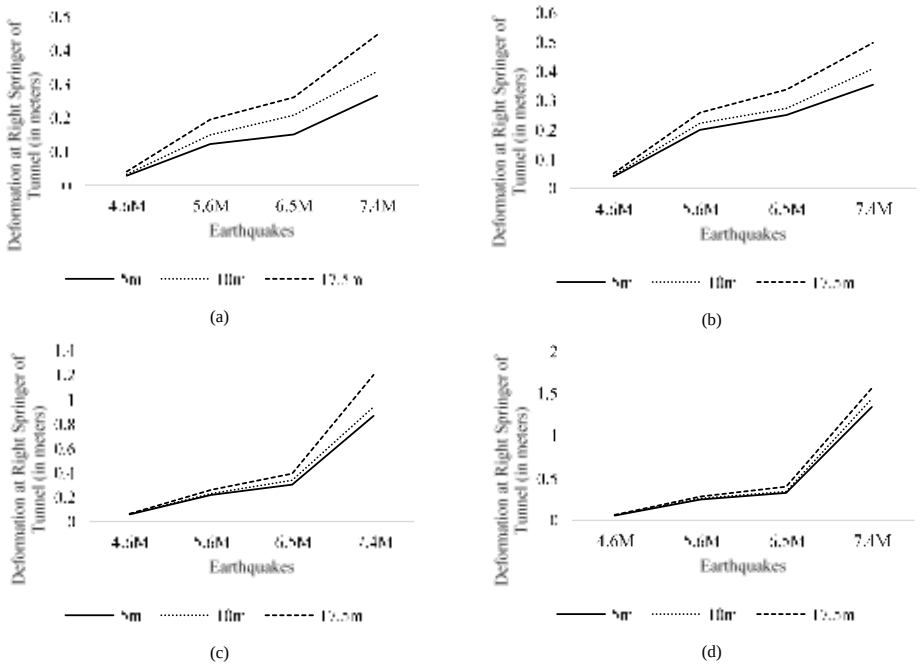

Fig. 7. Comparison of overburden depth for the different magnitude of earthquakes at right springer of the tunnel for (a) W0 (b) W1 (c) W2 and (d) W3 weathering stages of Basalt Rock.

Different magnitude earthquakes are compared in Figure 8 for different depths of overburden by plotting a graph between deformation and weathering stages of basalt rock. It can be seen that as the magnitude of the earthquake increases the deformation increases. In case of earthquakes except for major earthquake, the deformation varies at a particular rate which lies in a narrow zone of variation while in case of major earthquakes the deformation increases a faster rate as compared to another earthquake of different magnitude.

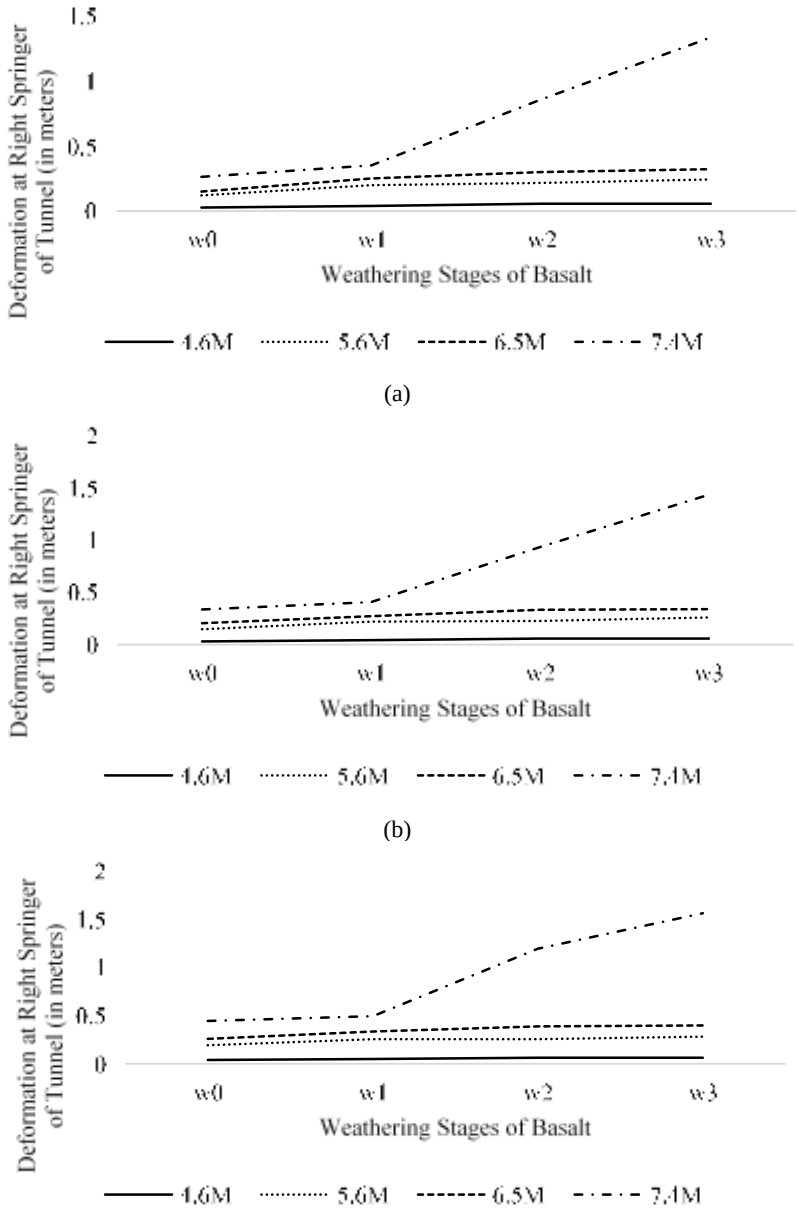

Fig. 8. Graph of deformation at right springer vs. weathering stages of basalt rock for the different magnitude of earthquakes for (a) 5m, (b) 10m, and (c) 17.5m depth of overburden.

4 Conclusion

A two-dimensional finite element analysis has been performed to study the behavior of rock tunnels considering weathering effects. Few important observations may be concluded as follows-

1. As the overburden pressure increases, the magnitude of deformation at crucial tunnel points reduces, thus, showing the effect of lithostatic condition.
2. The deformation increases as the weathering stage of the rock increases for each magnitude of earthquakes.
3. As the depth of overburden increases, the weathering has a significant effect on tunnel stability.
4. The overburden depth doesn't have much effect on the stability of the tunnel under the event of minor earthquakes while the overburden depth proved to be of greater significance in case of major earthquake events.
5. As anticipated, with the increase in the magnitude of the earthquake, the deformation increases.
6. In case of earthquakes except for major earthquake, the deformation varies at a definite rate which lies in a narrow zone of variation while in case of major earthquakes the deformation increases a faster rate as compared to another earthquake of different magnitude.

References

1. Zhang, D., Huang, Z., Li, Z., Zong, X. & Zhang, D. Analytical solution for the response of an existing tunnel to a new tunnel excavation underneath. Comput. Geotech. 108, 197–211 (2019).
2. Liu, X., Fang, Q., Zhang, D. & Wang, Z. Behaviour of existing tunnel due to new tunnel construction below. Comput. Geotech. 110, 71–81 (2019).
3. Jin, D., Yuan, D., Li, X. & Zheng, H. Analysis of the settlement of an existing tunnel induced by shield tunneling underneath. Tunn. Undergr. Sp. Technol. 81, 209–220 (2018).
4. Liu, X., Fang, Q. & Zhang, D. Mechanical responses of existing tunnel due to new tunnelling below without clearance. Tunn. Undergr. Sp. Technol. 80, 44–52 (2018).
5. Yeung, M. R. & Leong, L. L. EFFECTS OF JOINT ATTRIBUTES ON TUNNEL STABILITY. Int. J. Rock Mech. Min. Sci. 34, 3–4 (1997).
6. Zhang, J., Zhou, X. & Yin, P. Visco-plastic deformation analysis of rock tunnels based on fractional derivatives. Tunn. Undergr. Sp. Technol. 85, 209–219 (2019).
7. Manuello, A., Niccolini, G. & Carpinteri, A. Ae monitoring of a concrete arch road tunnel: damage evolution and localization. Eng. Fract. Mech. (2018). doi:10.1016/j.engfracmech.2018.07.029
8. Amouzandeh, A., Zeiml, M. & Lackner, R. Real-scale CFD simulations of fire in single- and double-track railway tunnels of arched and rectangular shape under different ventilation conditions. Eng. Struct. 1–14 (2014). doi:10.1016/j.engstruct.2014.05.027
9. Dancygier, A. N., Karinski, Y. S. & Chacha, A. A model to assess the response of an arched roof of a lined tunnel. Tunn. Undergr. Sp. Technol. 56, 211–225 (2016).

10. Masson, E. et al. Radio wave propagation in arch-shaped tunnels: Measurements and simulations by asymptotic methods. Comptes Rendus Phys. 11, 44–53 (2010).
11. LAI, J., FAN, H., LIU, B. & LIU, T. Analysis of Seismic Response of Shallow Large Section Multi-arch Tunnel. Adv. Control Eng. Inf. Sci. 15, 2–6 (2011).
12. Zhang, R., Xiao, Y., Zhao, M. & Zhao, H. Stability of dual circular tunnels in a rock mass subjected to surcharge loading. Comput. Geotech. 108, 257–268 (2019).
13. Do, N. & Dias, D. Tunnel lining design in multi-layered grounds. Tunn. Undergr. Sp. Technol. 81, 103–111 (2018).
14. Farhadian, H., Katibeh, H., Huggenberger, P. & Butscher, C. Optimum model extent for numerical simulation of tunnel inflow in fractured rock. Tunn. Undergr. Sp. Technol. 60, 21–29 (2016).
15. Kuo, K. A., Hunt, H. E. M. & Hussein, M. F. M. The effect of a twin tunnel on the propagation of ground-borne vibration from an underground railway. J. Sound Vib. 330, 6203–6222 (2011).
16. Lin, H., Xiang, Y., Yang, Y. & Chen, Z. Dynamic response analysis for submerged floating tunnel due to fluid-vehicle tunnel interaction. Ocean Eng. (2018). doi:10.1016/j.oceaneng.2018.08.023
17. Paternesi, A., Schweiger, H. F. & Scarpelli, G. Numerical analyses of stability and deformation behavior of reinforced and unreinforced tunnel faces. Comput. Geotech. 88, 256–266 (2017).
18. Su, K. et al. Transverse extent of numerical model for deep buried tunnel excavation. Tunn. Undergr. Sp. Technol. 84, 373–380 (2019).
19. Varma, M., Maji, V. B. & Boominathan, A. Numerical modeling of a tunnel in jointed rocks subjected to seismic loading. Undergr. Sp. 1–14 (2018). doi:10.1016/j.undsp.2018.11.001
20. Yang, J., Chen, W., Li, M., Tan, X. & Yu, J. Structural health monitoring and analysis of an underwater TBM tunnel. Tunn. Undergr. Sp. Technol. 82, 235–247 (2018).
21. Liu, L., Gao, Y., Liu, B. & Li, S. Preliminary seismic hazard assessment for the proposed Bohai Strait subsea tunnel based on scenario earthquake studies. J. Appl. Geophys. (2019). doi:10.1016/j.jappgeo.2019.02.005
22. Cheng, X., Xu, W., Yue, C., Du, X. & Dowding, C. H. Seismic response of fluid – structure interaction of undersea tunnel during bidirectional earthquake. Ocean Eng. 75, 64–70 (2014).
23. Miao, Y., Yao, E., Ruan, B. & Zhuang, H. Seismic response of shield tunnel subjected to spatially varying earthquake ground motions. Tunn. Undergr. Sp. Technol. 77, 216–226 (2018).
24. Zhao, W. et al. Earthquake input mechanism for time-domain analysis of tunnels in layered ground subjected to obliquely incident P- and SV-waves. Eng. Struct. 181, 374–386 (2019).
25. Lu, C. & Hwang, J. Damage analysis of the new Sanyi railway tunnel in the 1999 Chi-Chi earthquake : Necessity of second lining reinforcement. Tunn. Undergr. Sp. Technol. 73, 48–59 (2018).
26. Wang, Z. et al. Analysis of ground surface settlement induced by the construction of a large- diameter shallow-buried twin-tunnel in soft ground. Tunn. Undergr. Sp. Technol. 83, 520–532 (2019).
27. Fu, J., Yang, J., Zhang, X., Klapperich, H. & Muntazir, S. Response of the ground and adjacent buildings due to tunnelling in completely weathered granitic soil. Tunn. Undergr. Sp. Technol. 43, 377–388 (2014).

28. Wang, Z. L., Li, Y. C. & Shen, R. F. Numerical simulation of tensile damage and blast crater in brittle rock due to underground explosion. Int. J. Rock Mech. Min. Sci. 44, 730–738 (2007).
29. Shirlaw, J. N. Pressurised TBM tunnelling in mixed face conditions resulting from tropical weathering of igneous rock. Tunn. Undergr. Sp. Technol. 1–16 (2016). doi:10.1016/j.tust.2016.01.018
30. Nariman, N. A., Hussain, R. R. & Msekh, M. A. Prediction Meta-Models for the Responses of a Circular Tunnel During Earthquakes. Undergr. Sp. (2018). doi:10.1016/j.undsp.2018.06.003
31. Naqvi, M. W., Zaid, M., Sadique, R. & Alam, M. M. Dynamic Analysis of Rock Tunnels Considering Joint Dip Angle : a Finite Element Approach. in 13th International Conference on Vibration Problems (2017).
32. Zaid, M., Talib, A. & Sadique, M. R. Effect of joint orientation on the seismic stability of rock slope with transmission tower. in IGC-2018 (2018).
33. Gahoi, A., Zaid, M., Mishra, S. & Rao, K. S. Numerical Analysis of the Tunnels Subjected to Impact Loading. in INDOROCK (Indorock2017, 2017).
34. Zaid, M., Talib, A. & Md. Rehan Sadique. Stability Analysis of Rock Slope having Transmission Tower. IJRECE 6, (2018).
35. Zaid, M., Mishra, S. & Rao, K. S. Finite Element Analysis of Static Loading on Urban Tunnels. in IGC-2018 (2018).
36. Athar, M. F., Zaid, M. & Sadique, M. R. Stability of Different shapes of Tunnels in Weathering Stages of Basalt. in Proceedings of National Conference on Advances in Structural Technology 320–327 (2019).
37. Zaid, M., Khan, M. A. & Sadique, M. R. Dynamic Response of Weathered Jointed Rock Slope Having the Transmission Tower. in Proceedings of National Conference on Advances in Structural Technology 1, 414–422 (2019).
38. Zaid, M. & Sadique, M. R. Effect of Joint Orientation and Weathering on Static Stability of Rock Slope Having. in 7th Indian Young Geotechnical Engineers Conference – 7IYGEC 2019 15-16 March 2019, NIT Silchar, Assam, India SILCHAR (2019).
39. Mishra, S., Rao, S. & Gupta, N. K. Effect of different loading conditions on tunnel lining in soft rocks. in EUROCK 2016 (2016).
40. Mishra, S., Rao, K. S., Gupta, N. K. & Kumar, A. Damage to Shallow Tunnels under Static and Dynamic Loading. Procedia Eng. 173, 1322–1329 (2017).
41. Mishra, S., Rao, S., Gupta, N. K. & Kumar, A. Damage to shallow tunnels in different geomaterials under static and dynamic loading. Thin-Walled Struct. 126, 138–149 (2017).
42. Gupta, A. S. & Rao, K. S. Index properties of weathered rocks: inter-relationships and applicability. Bull. Eng. Geol. Environ. 57, 161–172 (1998).
43. Systems, C. of O. for S.-M. O. Strong Motion Virtual Data Center (VDC). (2018). Available at: https://strongmotioncenter.org/vdc/scripts/default.plx. (Accessed: 15th October 2018)